Finite Element Analysis on Burst Pressure of Defective Steel Pipes

N. A. Alang[1], N. A. Razak[2], K.A.Safie'[3], and A. Sulaiman[4]

Faculty of Mechanical Engineering, Universiti Malaysia Pahang, 26600, Pekan, Pahang Darul Makmur, Malaysia

[1]azuan@ump.edu.my, [2]norhaida@ump.edu.my, [3]azuwar@ump.edu.my,[4]syahrizan@ump.edu.my

Keywords: Ductile fracture simulation, Gouge, Stress modified critical strain, Stress triaxiality

Abstract. Pipelines are often subject to damages due to corrosion and third-party accidents such as gouges and dents. The effect of gouge depths on burst pressure of steel pipes was studied using a nonlinear finite element (FE) method combine with stress modified critical strain (SMCS) model. The procedure in determining the SMCS model parameters from smooth tensile bars is systematically discussed in this paper. The SMCS model was used to determine the burst pressure as a function of gouge depths of different pipe diameters. The burst pressure from FE was then compared with values calculated using design codes for pipelines containing defect. The FE results show the ratio of wall thickness to pipe diameter have significant influence on burst pressure.

Introduction

There are numerous design codes available in practice for prediction of failure pressure of defective pipe due to corrosion. Examples of the codes are American Society of Mechanical Engineer (ASME) B31G [1], modified ASME B31G [1] and DNV-RP-F101 [2]. However for gouge type defect, there are no reliable engineering assessment equations currently available. According to ASME B31G and DNV-RP-F101 codes, the failure of corroded pipeline is controlled by the defect size as well as the flow stress, S_f of the material. The input parameter including outer diameter of the pipe, D, wall thickness, t, yield strength of the material, σ_y or ultimate tensile strength, σ_u, the length of the defect, L and defect depth, d. The equations used to calculate the burst pressure, P_b based on these codes are expressed as:

$$P_b = \frac{2tS_f}{D} \tag{1}$$

For ASME B31G:

$$S_f = 1.1\sigma_y \left[\frac{1-\frac{2}{3}(\frac{d}{t})}{1-\frac{2}{3}(\frac{d}{t})/M}\right]; \qquad M = (1 + 0.8\frac{L^2}{Dt})^{0.5} \tag{2}$$

For Modified ASME B31G:

$$S_f = (\sigma_y + 69)\left[\frac{1-0.85\left(\frac{d}{t}\right)}{1-\frac{0.85\left(\frac{d}{t}\right)}{M}}\right]; \quad M = \left[1 + 0.6275\frac{L^2}{Dt} - 0.003375\left(\frac{L^2}{Dt}\right)\right]^{0.5} \tag{3}$$

For DNV-RP-F101:

$$P_b = 1.05\left(\frac{2t\sigma_u}{D-t}\right)\left[\frac{1-(\frac{d}{t})}{1-(\frac{d}{t})/M}\right]; \qquad M = \left[1 + 0.31\left(\frac{L^2}{Dt}\right)\right]^{0.5} \tag{4}$$

where *M* is bulging stress magnification factor.

All three codes use the stress based failure criterion to predict the burst pressure. This leads to conservative results because stress based failure criterion rely on flow stress only. Other method using strain based failure criteria which can be grouped into micro-mechanical models and cohesive zone models. Micro-mechanical model for ductile fracture, incorporating void nucleation, growth and coalescence are the Gurson–Tvergaard–Needleman (GTN) model [3], void growth model (VGM) [4], continuum damage model (CDM) [5,6], and SMCS [7-10] have been widely used over several decades. Results from these models [1-10] have been numerously published. Applicability and validity of these methods have been thoroughly discussed as well. However, a few issues need to be resolved in practical application of these methods. For example, GTN models consist of relatively high number of parameters compare to SMCS and VGM models [11]. These GTN parameters are difficult to identify and calibrate which requires a large number of FE and experimental work.

Kanvinde and Deierlein [12] compares both VGM and SMCS models in predicting the ductile failure of engineering structure made from structural steels. The results from Kanvinde and Deierlein conclude that both models can be applied accurately to the entire spectrum of structural steels in predicting ductile failure. However, the VGM requires tedious mathematical technique where the stress triaxiality and plastic strain history need to explicitly integrated. Mackenzie and Hancock [7] first developed the SMCS and reported that the model is a direct approach since the critical plastic strain as a function of stress triaxiality can be directly calculated. Due to its simplicity and accuracy, SMCS model is preferred by Oh et al [8-10] to predict the ductile failure of the materials. Mathematically, SMCS is evaluated by the Eq. (5) through Eq. (8), where the stress triaxiality, *T* is defined by the ratio of hydrostatic stress, σ_m and equivalent stress, σ_e given by:

$$T = \frac{\sigma_m}{\sigma_e} = \frac{\sigma_1+\sigma_2+\sigma_3}{3\sigma_e} \tag{5}$$

$$\sigma_e = \frac{1}{\sqrt{2}}[(\sigma_1-\sigma_2)^2 + (\sigma_3-\sigma_1)^2 + (\sigma_2-\sigma_3)^2]^{\frac{1}{2}} \tag{6}$$

On the other hand, the equivalent strain ε_e is given by:

$$\varepsilon_e = \frac{\sqrt{2}}{3}[(\varepsilon_1-\varepsilon_2)^2 + (\varepsilon_3-\varepsilon_1)^2 + (\varepsilon_2-\varepsilon_3)^2]^{\frac{1}{2}} \tag{7}$$

where the σ_1, σ_2, σ_3 and ε_1, ε_2, ε_3, are the principle stresses and principle strain respectively. The fracture strain ε_f is determined as follows using the equation proposed by Mackenzie and Hancock [7]:

$$\varepsilon_f = A\, exp\left(-\frac{3}{2}\frac{\sigma_m}{\sigma_e}\right) \tag{8}$$

where A is the material constant found through an experiment.

Oh et al [8] further developed SMCS failure criterion for API X65 steel pipes which is widely used for gas pipelines. The implementation by Oh calibrates the model using both smooth and notched tensile bar specimens. The burst pressure of defective pipes using SMCS failure criterion were compared with experimental results. The results [8] reported that the errors are less than 5% compared to experimental values. However, the work presented by Oh is only limited to pipe diameter of 762 mm and gouge depths of 8.75 mm.

The gouge depth damage on pipelines increases over the time that due to severity of corrosion [13], the study on it has significant important. Thus this study proposed to investigate this area in more detail. SMCS local failure criterion is applied to predict the burst pressure of defective API X42 pipeline steel. The SMCS model parameter was calibrated for the material studied for further simulation. The pipe with different gouge depth was modeled with commercial FE analysis software, MSC. Marc 2008r1. Finally, the burst pressure predicted from FE was then compared to existing pipe line code such as, ASME B31G, modified ASME B31G and DNV-RP-F101.

Material and Testing.

The material used in this study was API X42 steel [14]. Specimens for uniaxial tensile test were extracted in longitudinal direction from pipe schedule 120. A schematic diagram for tensile specimen used in this present work is illustrated in Fig.1. The tensile test was performed by following the ASTM E8-08 [15]. The tensile test was conducted at room temperature using universal testing machine Instron model 3369 having a load cell capacity of 50 kN equipped with personal computer. During the testing, an axial displacement was monitored using extensometer with 25 mm gauge length as shown in Fig 2. Engineering stress strain data was then converted to true stress strain data as plotted in Fig.3. Chemical compositions and mechanical properties of the material are tabulated in Table 1 and Table 2 respectively.

Table 1. Chemical composition of API X42 steel (%wt)

	C	P	Mn	S	Fe
Experimental	0.03	0.01	0.98	0.003	98.6
API Spec 5L [14]	0.28(max)	0.08(max)	1.3(max)	0.03(max)	Balance

Table 2. Mechanical properties of API X42 steel at room temperature

	Young Modulus, E (GPa)	Poisson Ratio, v	Yield Strength, σ_y (MPa)	Tensile Strength, σ_u (MPa)
Experimental	207	0.3	284.7	464.4

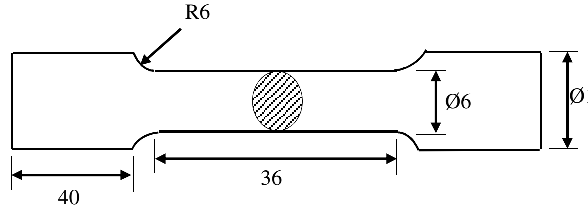

Fig.1. Tensile specimen.

Fig.2. Experimental set up for tensile specimen.

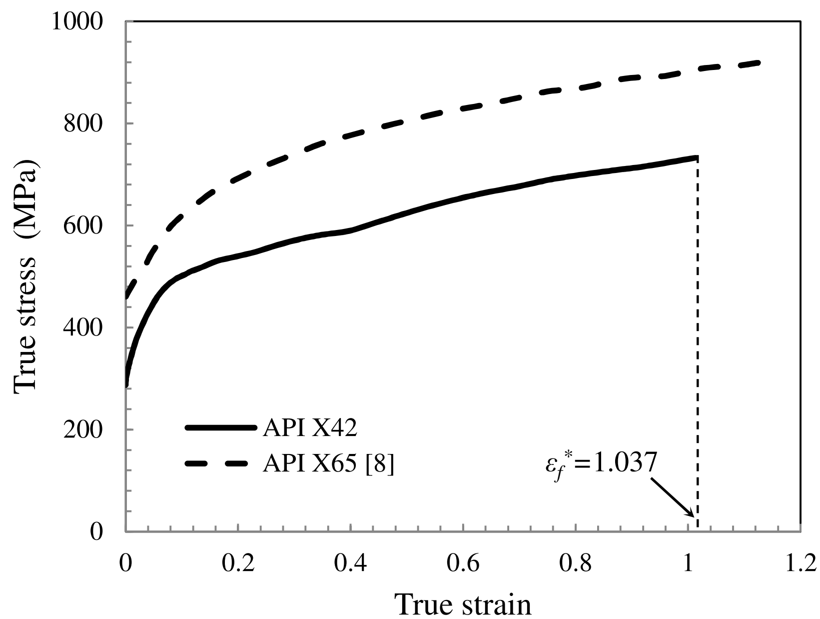

Fig. 3. True plastic stress-strain for API X42 data employed in FE analysis.

Finite Element Analysis

Fig. 4 shows schematic illustration of pipe with a gouge on its outer surface. The gouge is characterized by the 45 degree V-notch with the radius of 2 mm. The gouge length is denoted by *l* and the gouge depth is denoted by *d*. To investigate the effect of the gouge depth, nonlinear FE model of the pipe were performed using FE software, MSC Marc 2008r1. Detail finite element meshing is shown in Fig.5 together with enlargement view on the defective area. The boundary condition was applied at the end of the pipe to simulate the closed cap condition and the internal pressure was applied to the inner surface of the pipe. In all cases the symmetrical condition was utilized for computational efficiency. Therefore, only one quarter of the pipe was modeled. The material is model as an isotropic elasto-plastic material and the true stress strain data were employed. Three pipe diameters were selected, 508 mm, 762 mm and 1016 mm from piping data book [16]. To investigate the effect of gouge depth, three different ratio of gouge depth to thickness were selected. A total of nine cases were considered in this present work which is listed in Table 3.

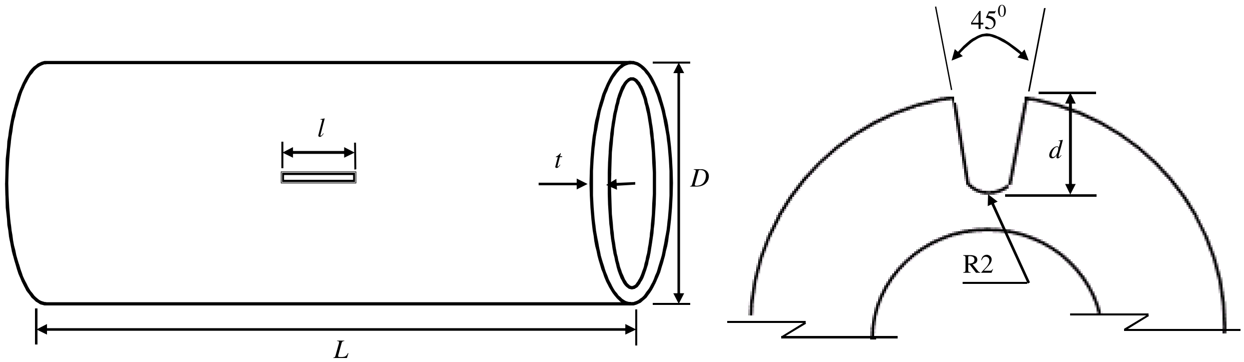

Fig. 4. Schematic of pipes with gouge defect.

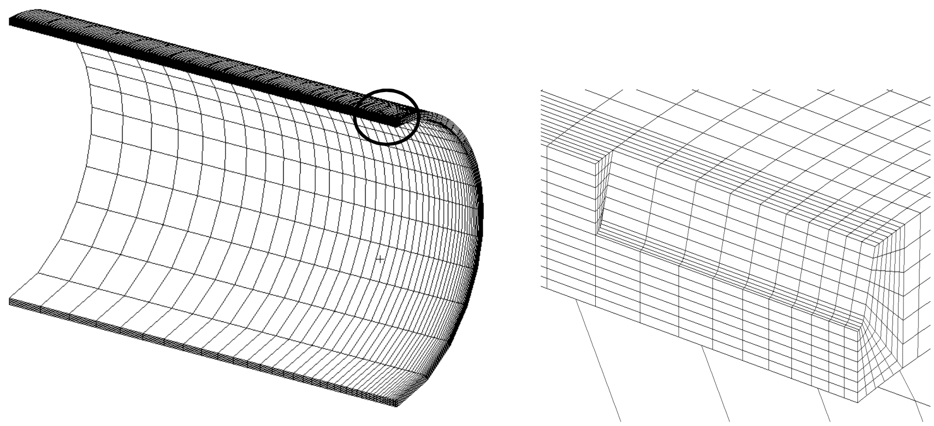

Fig. 5. Detailed mesh of the defective pipe used in FE analysis.

Table 3.Case analysis for pipe different pipe diameter and gouge depth.

Pipe diameter, D (mm)	Gouge length, l (mm)	Gouge depth, d (mm)
508, 762, 1016	100	4.375, 8.75, 13.125

Determination of Stress Modified Critical Strain Model Parameter

Remarking that the stress triaxiality for round bars is roughly $\sigma_m/\sigma_e \approx 1/3$ [17] and an approximate expression of the ratio of fracture strain ε_f for the same material is given by:

$$\frac{\varepsilon_f}{\varepsilon_f^*} = \frac{exp\left(\frac{-3\sigma_m}{2\ \sigma_e}\right)}{exp(-0.5)} \quad (10)$$

where ε_f^* denotes the fracture strain obtained from tensile test of smooth round bar. In the present work, the fracture strain obtained from an average of three tensile smooth round bar is $\varepsilon_f^* = 1.037$ as shown in Fig.3 and thus the ε_f for API X42 material used in this paper is proposed to be:

$$\varepsilon_f = 1.732\, exp\left(-1.5\frac{\sigma_m}{\sigma_e}\right) \quad (11)$$

For comparison Oh et al. [8] had used Eq. (12) for API X65 is:

$$\varepsilon_f = 3.29\, exp\left(-1.54\frac{\sigma_m}{\sigma_e}\right) + 0.10 \quad (12)$$

Note that in Eq. (12) Oh et al. had included a value of 0.10 in the last parameter. This value represents the plastic flow that occurs before voids nucleate which is not included in this present work.

In order to predict the burst pressure of defective pipes using the present approaches, the proposed equation, Eq. (11) was combined with detailed nonlinear elasto-plastic FE analyses from which notch tip stresses and strains are determined. For instance, from the FE analysis, stress and strain information can be monitored as a function of load. Over the loading history, the stress triaxiality and equivalent strain were calculated using Eq. (5) to (7) for every time step. When the equivalent strain from the FE analysis equals to the fracture strain, the failure is assumed to occur.

Fig. 6.0 summarizes the resulting true fracture strain,ε_f as a function of the stress triaxiality for both API X65 and API X42 steels. For API X65, the equation for fracture strain was proposed by Oh et al. [8]. The true fracture strain can be represented as an exponentially dependent on the stress triaxiality [7]. Based on the Fig 4.0, it is noted that the true fracture strain for API X42 is lower compared to API X65 as proposed by Oh et al. [8].

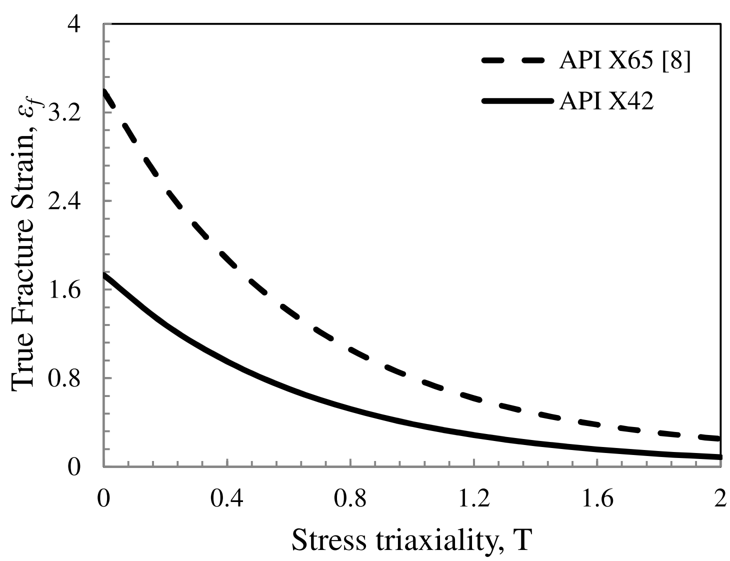

Fig. 6.0. True fracture strain as a function of stress triaxiality.

Results

Effect of Gouge Depth on Burst Pressure. Table 4 represents the predicted burst pressure results obtained from FE analysis. The results show that the burst pressure decreases with increasing pipe diameters and gouge depths. The burst pressure results for intact pipe was also included for comparative purposes between stress-based and strain-based criteria. The burst pressure for intact pipe was calculated using Eq. (13). This equation is based on stress criterion which applies tensile strength, σ_u as a maximum allowable stress of the pipes. It is clearly shown in Table 4, the burst pressure of intact pipe is lower than the value of burst pressure obtained using FE model for gouge depth of 4.375 mm. This is due to different approaches implemented for stress-based and strain-based criteria. Furthermore, the strain-based criteria that was applied in this study took into consideration the increment of the pressure beyond the onset of necking. In contrast, stress-based criterion for Eq. (13) neglecting the remaining pressure at the uniform strain up to fracture point.

$$P_b = \frac{2t\sigma_u}{(D-2t)} \tag{13}$$

Fig. 7 shows a plot of burst pressure as a function of gouge depth for API X65 and API X42. It is shown that the burst pressure between pipe diameter 762 mm and 1016 mm have no significant different. However, when the pipe diameter decreases to 508 mm, burst pressure rise dramatically. This is due to the ratio of wall thickness to pipe diameter is largest for the pipe with D = 508 mm. The results also shown that the burst pressure of defective pipe tends to level out when the gouge depth are greater than 8.75 mm.

Table 4. Summary of Burst Pressure Prediction of API X42 steel pipe.

Case No.	Pipe Diameter, (mm)	*t/D* (%)	Defect Dimension, (mm)			Burst Pressure	Intact Burst Pressure
			Depth, *d*	*d/t*	Length, *l*		
CS1	508	3.44	4.375	0.25	100	34.8	34.4
CS2			8.75	0.5		28.8	
CS3			13.125	0.75		20.8	
CS4	762	2.29	4.375	0.25		24.0	22.4
CS5			8.75	0.5		19.2	
CS6			13.125	0.75		15.6	
CS7	1016	1.72	4.375	0.25		18.4	16.6
CS8			8.75	0.5		16.8	
CS9			13.125	0.75		13.8	

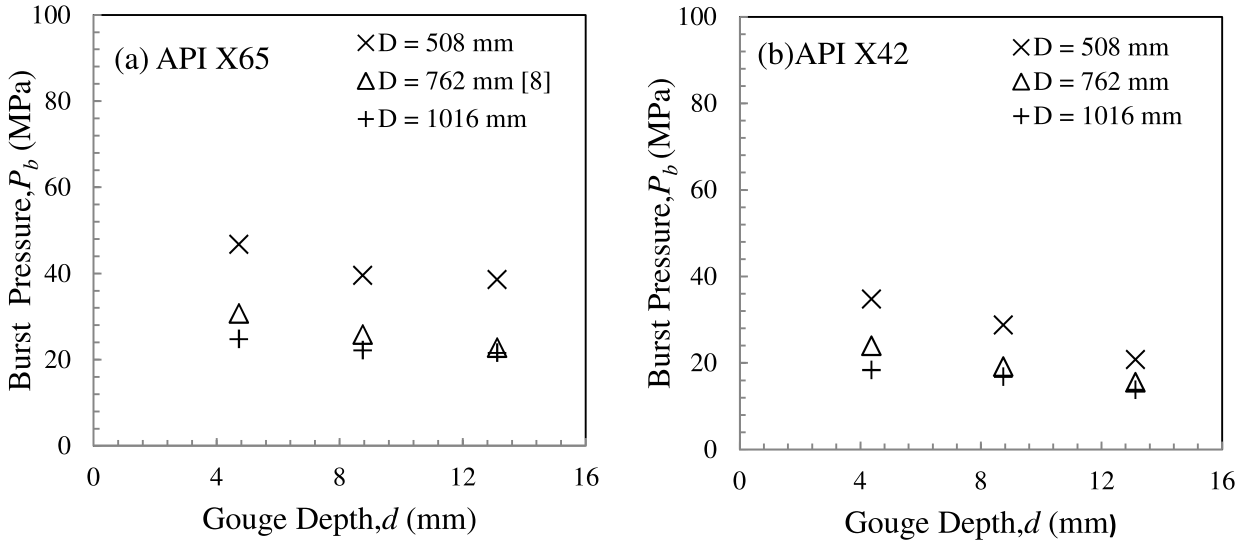

Fig. 7. Relationship between burst pressure and gouge depth for (a) API X65 and (b) API X42

Comparison between FE Results and Available Codes for Pipeline Defect Assessment. For the purpose of comparison, the gouge will be assumed to be as a part of corrosion defect. Fig.8 compares the results for the burst pressure between the available codes and FE for outer diameter of 1016 mm. The most conservative code in predicting the burst pressure is ASME B31G followed by modified ASME B31G and DNV-RP-F101. This is certainly true for all cases studied except for CS9-API X65. In contrast, FE results shows higher values as compare to other codes except for CS9-API X42 where DNV-RP-F101 code appear to be highest. It is might due to limitation of the DNV-RP-F101 code that only applicable for ratio of gouge depth to pipe thickness less or equal to 70%. It is noted that all three codes predict the failure based on stress criterion where the flow stress govern the predicted results whereas the burst pressure obtained from FE analysis is based on strain criterion.

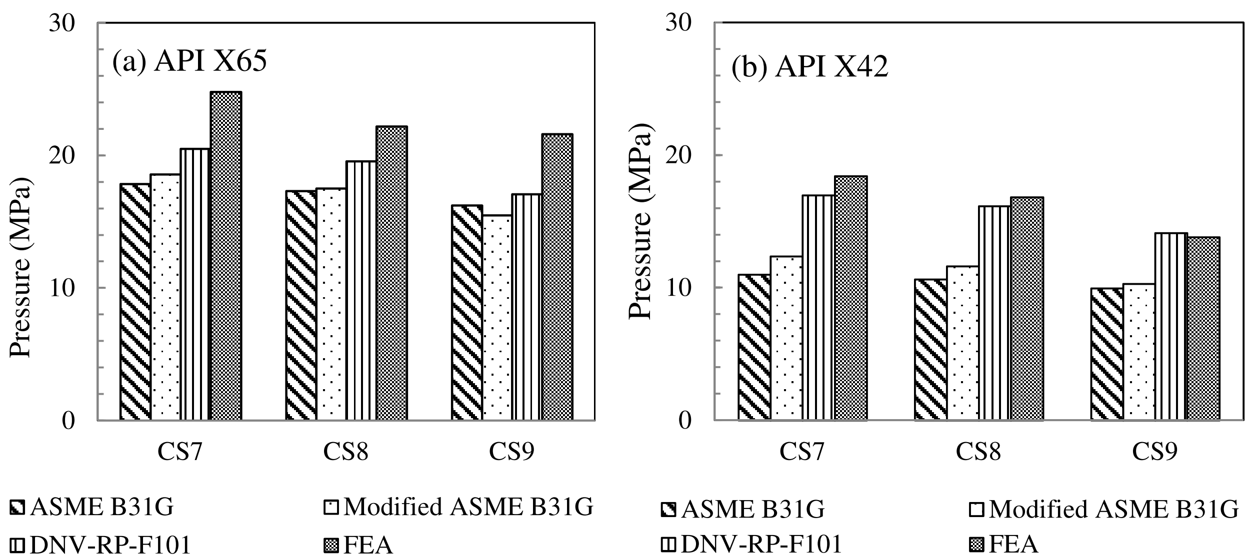

Fig. 8. Predicted burst pressure for D = 1016 mm; (a) API X65 and, (b) API X42

Conclusion

The burst pressure of defective pipes API X42 and API X65 with different gouge depth and diameter was successfully predicted using nonlinear FE analysis by implementing the SMCS model. The FE results were then compared to available pipeline design code. The following conclusion can be drawn:

1) The burst pressure decreases as the gouge depth increases. The burst pressure drop rapidly when the pipe diameter increase from 508 mm to 762 mm. However, there is no significant different on burst pressure as the pipe diameter change from 762 mm to 1016 mm. The reason is owing to the influence of the ratio of wall thickness to pipe diameter.
2) The FE results based on strain based criterion always give higher value of burst pressure than other codes that apply stress criterion.

References

[1] ASME B31G-2009. Manual for determining the remaining strength of corroded pipelines. A supplement to ASME B31 code for pressure piping. (1991)

[2] DNV Recommended Practice, RP-F101. Corroded pipelines, Det Norske Veritas. October, (2010)

[3] AL Gurson , Continuum theory of ductile rupture by void nucleation and growth. Part 1- yield criteria and flow rules for porous ductile media. J Eng Mater Tech 1(977)

[4] J. R. Rice, D. Ai. Tracey, On The Ductile Enlargement of Voids In Triaxial Stress Fields, J. Mech. Phys. Solids, (1969), Vol. 17, pp. 201 to 217.

[5] J.A Lemaitre, Continuous Damage Mechanics Model for Ductile Fracture. Journal of Engineering Material and Technology 107, 83-89. (1985)

[6] Nicola Bonora , Domenico Gentile, A. Pirondi, Golam Newaz ,Ductile damage evolution under triaxial state of stress: theory and experiments, , International Journal of Plasticity 21 (2005) 981–1007

[7] A. C. Mackenzie, J. W. Hancock and D. K. Brown , On The Influence of State of Stress on Ductile Failure Initiation In High Strength Steels, Int J Fract Mech (1977)

[8] C.K.Oh , Y.J. Kim, J.H Baek , W.-s.Kim : Development of Stress-Modified Fracture Strain for Ductile Failure of API X65 steel. Int J Fract (2007);143:119–33.

[9] C.K.Oh , Y.J. Kim, J.H Baek , W.-s.Kim ,A Finite Element Ductile Failure Simulation Method using Stress-Modified Fracture Strain Model", Int J Fract (2011) 78:124–137

[10] C.K.Oh , Y.J. Kim, J.H Baek , W.-s.Kim, Ductile Failure Analysis of API X65 pipes with Notch-Type Defects using a Local Fracture Criterion , Int J of Pressure Vessels and Piping 84 (2007) 512–525

[11] C.K.Oh , Y.J. Kim, J.H Baek , Y.P.Kim, W.-s.Kim,A phenomenological model of ductile fracture for API X65 steel, Int.Journal of Mechanical Sciences 49, 1399-1412, (2007)

[12] A. M. Kanvinde and G.G Deierlein, The Void Growth Model and The Stress Modified Critical Strain Model To Predict Ductile Fracture In Structural Steels. (2005)

[13] T.A. Netto, U.S. Ferraz, S.F. Estefen, The effect of corrosion defects on the burst pressure of pipelines, Journal of Constructional Steel Research, 61, (2005) 1185–1204

[14] API Spec 5L, Specification for Line Pipe, 42nd Edition, American Petroleum Institute (2000)

[15] ASTM Standard E8-08, Standard Test Method for Tension Testing of Metallic Material. American and Society for Testing and Materials. (2008)

[16] L.Nayyar, Piping Databook (1996)

[17] P.W. Bridgman, Trans. Am. Society Material, Vol.32, p.553,(1944)